Cluster Chemistry with Sulfur-Containing Ligands: Reactions of the Hexanuclear Cluster (μ_2-H)Ru$_6$(CO)$_{16}$(μ_5-S)(μ_3,η^2-SCNHPhNPh) with Two-Electron-Donor Ligands

Lisa A. Hoferkamp, Gerd Rheinwald, Helen Stoeckli-Evans, and
Georg Süss-Fink*

*Institut de Chimie, Universitè de Neuchâtel, Avenue de Bellevaux 51,
CH-2000 Neuchâtel, Switzerland*

The reaction of the hexanuclear cluster (μ_2-H)Ru$_6$(CO)$_{16}$(μ_5-S)(μ_3,η^2-SCNHPhNPh) (**1**) with triphenylphosphine mainly results in the formation of the substitution product (μ_2-H)Ru$_6$-(CO)$_{15}$(PPh$_3$)(μ_5-S)(μ_3,η^2-SCNHPhNPh) (**3**). X-ray structural analysis of a single crystal of **3** identified the site of substitution as the apical, S-bound Ru atom of the starting cluster and revealed a significant degree of cluster deformation upon substitution. Crystals of **3** are triclinic, space group $P\bar{1}$: $Z = 2$, $a = 9.808(2)$ Å, $b = 10.285(2)$ Å, $c = 27.48(1)$ Å, $\alpha = 91.97(2)°$, $\beta = 90.02(2)°$, $\gamma = 94.52(2)°$. Reactions of **1** with other two-electron-donor ligands [Me$_2$S, P(n-Bu)$_3$, P(OMe)$_3$, P(OPh)$_3$, and ^{t}BuNC] also resulted in the substitution of a carbonyl group to give (μ_2-H)Ru$_6$(CO)$_{15}$(L)(μ_5-S)(μ_3,η^2-SCNHPhNPh) [L = Me$_2$S, **4**; P(n-Bu)$_3$, **5**; P(OMe)$_3$, **6**; P(OPh)$_3$, **7**; ^{t}BuNC, **8**]. The spectra of these substitution products differ from those of **3**, indicating an alternative site of substitution. This was verified through X-ray structural analysis of the ^{t}BuNC derivative **8**, which showed the isonitrile ligand to occupy an axial site on the apical Ru atom at the end of the cluster opposite to that found in **3**. Crystals of **8** are triclinic, space group $P\bar{1}$: $Z = 2$, $a = 9.431(2)$ Å, $b = 15.794(2)$ Å, $c = 16.772(2)$ Å, $\alpha = 87.94(1)°$, $\beta = 84.72(1)°$, $\gamma = 76.70(1)°$.

Introduction

Cotton's general definition of a metal cluster as a group of two or more metal atoms in which substantial bonding occurs among the metals[1] is useful in differentiating clusters from Werner-type coordination complexes. In many of the later reviews of metal clusters, however, this definition is narrowed to include only those species containing at least three metal atoms. The next step, from metal clusters to metal surfaces, is a more difficult distinction. The point at which one passes from a nonmetallic state to a metallic state has been the subject of considerable research.[2] Localized versus delocalized bonding within the metal framework provides a starting point. It has been shown that when cluster nuclearity approaches six metal atoms, a localized bonding description no longer provides an adequate description.[3] At this point, a delocalized bonding approach, more similar in nature to the band theory of metals, becomes necessary. Given such a position within the cluster hierarchy, the types of reactions and transformations undertaken by hexanuclear clusters offer a simplified model of those processes at the metal surface.

The full range of structural motifs displayed by hexanuclear cluster compounds is well-documented.[4] The relationships between the observed geometries of these clusters and their closed-shell electronic requirements comprise a large portion of the polyhedral

skeletal electron pair theory (PSEPT).[5] The majority of M$_6$ clusters adopt an octahedral geometry; therefore, not surprisingly, clusters of this type were among the first to be isolated and structurally characterized. The 86-electron octahedral cluster Ru$_6$C(CO)$_{17}$ is a typical example.[6] Many clusters have been isolated whose geometries are derived from standard polyhedra by capping or bridging to provide the additional vertices necessary to accommodate the additional metal atoms. These include the bicapped tetrahedral geometry and the capped square pyramid, as exemplified by Os$_6$(CO)$_{17}$-(MeCN) and Os$_6$(CO)$_{17}$(μ_4,η^2-HCCEt), respectively.[7] These clusters contain a total of 84 and 86 valence electrons, respectively, which are the numbers predicted from PSEPT. As opposed to the addition of vertices, the structures of some hexanuclear clusters must be considered as larger polyhedra with vertices missing, as in the case of the edge-bridged diminished pentagonal bipyramid found for (μ_2-H)Ru$_6$C(CO)$_{15}$(SEt)$_3$.[8] Analogous to the boranes and carboranes, the opening up of the polyhedral geometry requires additional skeletal electrons; thus, the edge-bridged diminished pentagonal bipyramid shows an electron count of 92 electrons. Further variations are planar raft structures including

⊗ Abstract published in *Advance ACS Abstracts,* January 15, 1996.
(1) Cotton, F. A. *Q. Rev.* **1966**, *20*, 389.
(2) Schmid, G. *Struct. Bond.* **1985**, *62*, Chapter 2.
(3) Mingos, D. M. P.; Wales, D. J. In *Introduction to Cluster Chemistry*; Grimes, R. N., Ed.; Prentice Hall International Editions Inc.: Englewood Cliffs, NJ, 1990; Chapter 2.

(4) (a) Ma, L.; Williams, G. K.; Shapley, J. R. *Coord. Chem. Rev.* **1993**, *128*, 261. (b) *Metal Clusters*; Moskovits, M., Ed.; John Wiley & Sons: New York, 1986.
(5) (a) Williams, R. E. *Prog. Inorg. Chem. Radiochem.* **1976**, *18*, 67. (b) Wade, K. *Adv. Inorg. Chem. Radiochem.* **1976**, *18*, 1. (c) Mingos, D. M. P. *Acc. Chem. Res.* **1984**, *17*, 311. (d) Rudolph, R. W. *Acc. Chem. Res.* **1976**, *9*, 446.
(6) Johnson, B. F. G.; Johnston, R. D.; Lewis, J. *J. Chem. Soc. A* **1968**, 2856.
(7) Gomez-Sal, M. P.; Johnson, B. F. G.; Kamarudin, R. A.; Lewis, J.; Raithby, J. *J. Chem. Soc., Chem. Commun.* **1985**, *1622*.
(8) Johnson, B. F. G.; Lewis, J.; Wong, K.; McPartlin, M. *J. Organomet. Chem.* **1980**, *185*, C17.

both the triangular raft, $[(\mu_3\text{-H})Ru_6(CO)_{15}(\mu_3\text{-S})_3]^-$ (ref 11d), and the rhombic raft cluster, $(\mu_2\text{-H})_4(\mu_3\text{-H})_2Ru_6$-$(CO)_{14}(\mu_3,\eta^2\text{-ampy})_2$.[9] The former cluster contains 92 valence electrons, which is 2 greater than the number predicted from PSEPT. This feature has been used to explain the elongation of certain M−M bonds via the population of antibonding cluster orbitals.[10] The latter cluster also contains 92 valence electrons, but this is in accord with its geometry. Distortion of the metal plane of the rhombic raft cluster results in alternative core configurations. Some of these configurations resemble the various conformers of cyclohexane,[11] while others represent structural intermediates between the stable conformations.[12] The majority of these latter raft-type clusters are either electron-rich or electron-precise, and all contain multiply bridging ligands.

From a simple thermolysis reaction of the trinuclear cluster $(\mu_2\text{-H})Ru_3(CO)_9(\mu_3,\eta^2\text{-SCNHPhNPh})$,[13] it was possible to isolate two hexanuclear thioureato clusters, each with a metal skeleton that mimics a known conformer of cyclohexane. The first of these is structurally similar to the *boat* conformer, $Ru_6(\mu_2\text{-CO})_2(CO)_{14}$-$(\mu_4\text{-S})(\mu_3,\eta^2\text{-NPhCNHPh})(\mu_3,\eta^2\text{-SCNHPhNPh})$, while the second is a structural analogue of the *sofa* conformer, $(\mu_2\text{-H})Ru_6(CO)_{16}(\mu_5\text{-S})(\mu_3,\eta^2\text{-SCNHPhNPh})$ (**1**). The sofa-like structure is produced in relatively high yield (46%) for a preparative procedure that is known for its lack of selectivity. Given the easy access to reasonable amounts of the second hexanuclear species, it was considered an ideal opportunity to explore its reactivity toward a series of organic reagents.
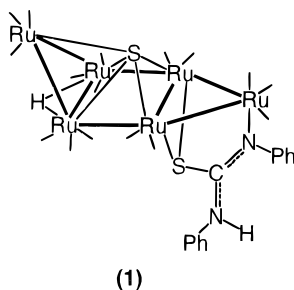

(1)

Results and Discussion

Reaction of $(\mu_2\text{-H})Ru_6(CO)_{16}(\mu_5\text{-S})(\mu_3,\eta^2\text{-SCNHPh-}$ NPh) (1) with Triphenylphosphine. Reaction of **1** with 1 or 2 equiv of PPh$_3$ over a period of 12 h, at 20 °C in dichloromethane or cyclohexane, gave three different products. Preparative TLC separated these compounds, in order of elution, as a bright red band, a yellow band, and a brick red band. The bright red band was identified by its IR spectrum as the compound $Ru_3(CO)_6$-$(\mu_2,\eta^2\text{-C}_6H_5)(PPh_3)(\mu_2\text{-PPh}_2)(\mu_3\text{-S})$. This same trinuclear cluster is available from thermal reactions of the tri-

nuclear cluster $(\mu_2\text{-H})Ru_3(CO)_9(\mu_3,\eta^2\text{-SCNHPhNPh})$ with 2 equiv of PPh$_3$ or direct thermolysis of the disubstituted derivative $(\mu_2\text{-H})Ru_3(CO)_7(PPh_3)_2(\mu_3,\eta^2\text{-SCNHPhNPh})$.[14] The IR and NMR data distinguished the yellow band as a dinuclear Ru complex with the formula $Ru_2(CO)_4$-$(PPh_3)_2(\mu_3,\eta^2\text{-SCNHPhNPh})$ (**2**). Spectral data indicated the brick red compound to be the monosubstituted, PPh$_3$ derivative of **1**, $(\mu_2\text{-H})Ru_6(CO)_{15}(PPh_3)(\mu_5\text{-S})(\mu_3,\eta^2\text{-SCN-}$ HPhNPh) (**3**).

Symmetrically substituted, dinuclear Ru complexes have been isolated and characterized previously.[15] The carbonyl region of IR and both ^{1}H and ^{31}P NMR spectra of **2** are consistent with a complex of this type, and, on the basis of these data, compound **2** is identified as Ru_2-$(CO)_2(SCNHPhNPh)_2$. In compound **2**, two diphenyl-
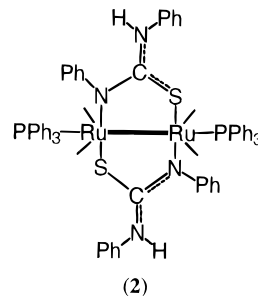
(2)

thioureato ligands span the Ru−Ru vector, bonding in a terminal fashion through the S and the N. One PPh$_3$ and two carbonyl ligands are terminally bonded to each Ru atom. Only the N−H stretch in the IR spectrum of **2** was not identifiable. If the diphenylthioureato ligand is considered a three-electron donor, then the dinuclear species **2** is electron-precise with a total of 34 valence electrons.

Spectroscopic data for **3** show a relatively simple carbonyl region; only five bands are observed. The presence of an undisturbed diphenylthioureato ligand is clear from IR and ^{1}H NMR data. Integration of the phenyl and the NH regions of the ^{1}H NMR spectrum, combined with the ^{31}P NMR spectrum, leads to a single, σ-bonded PPh$_3$ group. Room temperature ^{1}H NMR spectra of **3** in CDCl$_3$ show a broad, poorly defined peak in the hydride region (−17.50 ppm). The downfield shift of the signal relative to that of **1** (−22.0 ppm) suggests a chemical environment for this proton that is less affected by the anisotropy of the metal core. Upon cooling of a CD$_2$Cl$_2$ sample to −70 °C, two well-defined singlets at −17.70 and −17.73 ppm (400 MHz) in an approximately 1:1 ratio are observed. This result is consistent with the presence of two interconverting isomers in room temperature solutions of **3**.
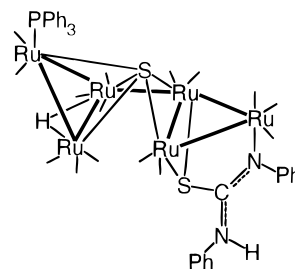
(3)

An X-ray structural characterization of **3** provided the exact location of the PPh$_3$ ligand on the hexanuclear framework and also revealed some interesting struc-

(9) (a) Cifuentes, M. P.; Jeynes, T. P.; Humphrey, M. G.; Skelton, B. W.; White, A. H. *J. Chem. Soc., Dalton Trans.* **1994**, 925. (b) Cabeza, J. A.; Fernández-Colinas, F. M.; García-Granda, S.; Llamazares, A.; López-Ortíz, F; Riera, V.; Van der Maelen, J. F. *Organometallics* **1994**, *13*, 426.

(10) Boag, N. M.; Knobler, C. B.; Kaesz, G. D. *Angew. Chem., Int. Ed. Engl.* **1983**, *22*, 249.

(11) (a) Gervasio, G.; Rossetti, R.; Stanghellini, P. L.; Bor, G. *Inorg. Chem.* **1984**, *23*, 2073. (b) Adams, R. D.; Babin, J. E.; Tasi, M. *Inorg. Chem.* **1987**, *26*, 2561. (c) Cockerton, B. R.; Deeming, A. *Polyhedron* **1994**, *13* (13), 2085. (d) Bodensieck, U.; Hoferkamp, L.; Stoeckli-Evans, H.; Süss-Fink, G. *J. Chem. Soc., Dalton Trans.* **1993**, 127.

(12) Jeannin, S.; Jeannin, Y.; Robert, F.; Rosenberger, C. *Inorg. Chem.* **1994**, *33*, 243.

(13) Hoferkamp, L.; Rheinwald, G.; Stoeckli-Evans, H.; Süss-Fink, G. *Inorg. Chem.* **1995**, in press.

Table 1.   Crystallographic Data for Clusters 3 and 8[a]

	compound	
	3	**8**
molecular formula	$C_{46}H_{26}N_2O_{15}PRu_6CH_2Cl_2$	$C_{33}H_{20}N_3O_{15}Ru_6S_2 \cdot C_{1.5}O_{0.5}$
MW	1633.1	1398.1
Z	2	2
crystal dimensions (mm)	$0.38 \times 0.38 \times 0.15$	$0.72 \times 0.42 \times 0.06$
crystal color/habit	deep red/plates	red/plates
crystal system	triclinic	triclinic
space group	$P\bar{1}$	$P\bar{1}$
a (Å)	9.808(2)	9.431(2)
b (Å)	10.285(2)	15.794(2)
c (Å)	27.48(1)	16.772(2)
α (deg)	91.97(2)	87.94(1)
β (deg)	90.02(2)	84.72(1)
γ (deg)	94.52(2)	76.70(1)
V (Å^3)	2761.8(13)	2420.6(7)
D_c (g cm^{-3})	1.964	1.928
μ(Mo Kα) (mm^{-1})	3.66	1.827
T of data collection (°C)	-60	20
$F(000)$	3104	1346
absorption correction	empirical/psi scans	empirical/difabs
T_{max}/T_{min}	0.4833/0.2971	1.000/0.227
no. of unique data	9724	8485
no. of obs. data used [$F_o > 2.5\sigma(F_o)$]	7123	8483
$2\theta_{min}/2\theta_{max}$ (deg)	3/50	3/50
$R(R')^{b,c}$	0.039 (0.052)	
$R(>2\sigma F^2)/R_1$(all)^{d,e}		0.071 (0.131)
$wR_2(>2\sigma F^2)/wR_2$(all)^f		0.171 (0.193)
residual electron density difference features (max/min) (e Å^{-3})	1.29/-1.21	1.397/-1.203

^{a} Details in common: data were collected on a Stoe-Siemens AED 2 four-circle diffractometer; graphite-monochromated Mo Kα radiation, $\lambda = 0.710\,73$ Å; scan mode $\omega - \theta$. ^{b} Refinement was by full-matrix least squares with a weighting scheme of the form $w^{-1} = \sigma^2(F_o) + k(F_o^2)$. ^{c} $R = \sum||F_o| - |F_c||/\sum|F_o|$, $R' = [\sum w(|F_o| - |F_c|)^2/\sum w(|F_o|)^2]^{1/2}$. ^{d} Structure refinement was carried out by using SHELXL93. ^{e} $R = \sum||F_o| - |F_c||/\sum|F_o|$. ^{f} $wR_2 = [\{\sum[w(F_o^2 - F_c^2)^2]/\sum[w(F_o)^4]\}]^{1/2}$, $w^{-1} = [\sigma^2(F_o^2) + (waP)^2 + wbP]$, $P = (F_o^2 + 2F_c^2)$.
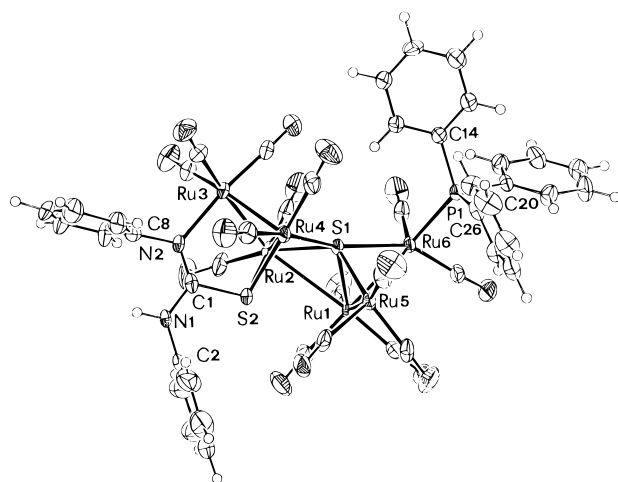
Figure 1. Molecular structure of **3**.

tural features. Deep red plates of **3** were grown from CH$_2$Cl$_2$/hexanes solutions. Crystals of **3** are triclinic and belong to the space group $P\bar{1}$, $Z = 2$. Additional crystal data are available in Table 1. The molecular structure of **3** is illustrated in Figure 1, while selected bond lengths and angles are summarized in Table 2. The metal framework of **3** consists of six Ru atoms, arranged analogously to those of **1**. A pentacoordinate sulfur ligand S1 remains bonded through five σ-bonds to Ru1, Ru2, Ru4, Ru5, and Ru6. A μ_3,η^2-diphenylthioureato ligand spans the Ru2–Ru4 triangular substructure; the S (S2) bridges Ru2 and Ru4, and the N (N2) is bound terminally to Ru3. An apical CO ligand on Ru6 has been replaced with a PPh$_3$ ligand. An appropriate number of terminal CO ligands were located on each of the six Ru atoms.

However, the original sofa-like configuration of **1** has been somewhat distorted in **3**. The distance between Ru1 and Ru2 (3.3729(11) Å) has increased by *ca.* 0.20 Å from that of **1** (3.1713(6) Å). While, in general, M–M

Table 2.   Selected Bond Lengths (Å) and Angles (deg) for 3

Ru(1)–Ru(5)	2.7904(10)	Ru(5)–Ru(6)	2.7885(11)
Ru(1)–Ru(6)	2.9529(10)	Ru(5)–S(1)	2.3646(16)
Ru(1)–S(1)	2.3762(17)	Ru(6)–P(1)	2.3743(18)
Ru(2)–Ru(3)	2.7206(10)	Ru(6)–S(1)	2.3381(18)
Ru(2)–Ru(4)	2.9106(10)	P(1)–C(14)	1.816(6)
Ru(2)–S(1)	2.4089(17)	P(1)–C(20)	1.835(6)
Ru(2)–S(2)	2.4287(18)	P(1)–C(26)	1.830(7)
Ru(3)–Ru(4)	2.7100(10)	S(2)–C(1)	1.781(7)
Ru(3)–N(2)	2.164(5)	N(1)–C(2)	1.417(9)
Ru(4)–Ru(5)	3.0870(11)	N(2)–C(1)	1.272(9)
Ru(4)–S(1)	2.4285(18)	N(2)–C(8)	1.452(9)
Ru(4)–S(2)	2.4091(19)	C(1)–N(1)	1.362(9)
Ru(1)–Ru(2)–Ru(3)	143.01(3)	Ru(3)–Ru(4)–Ru(5)	148.62(3)
Ru(1)–Ru(2)–Ru(4)	86.12(3)	Ru(3)–N(2)–C(1)	121.6(4)
Ru(1)–Ru(5)–Ru(4)	94.01(3)	Ru(3)–N(2)–C(8)	119.1(4)
Ru(1)–Ru(5)–Ru(6)	63.92(3)	Ru(4)–Ru(5)–Ru(6)	96.87(3)
Ru(1)–Ru(6)–Ru(5)	58.07(3)	Ru(4)–S(1)–Ru(5)	80.18(5)
Ru(1)–S(1)–Ru(2)	89.64(6)	Ru(4)–S(2)–C(1)	103.48(24)
Ru(1)–S(1)–Ru(6)	77.56(5)	Ru(5)–Ru(1)–Ru(6)	58.011(24)
Ru(2)–Ru(1)–Ru(5)	88.11(3)	Ru(5)–S(1)–Ru(6)	72.73(5)
Ru(2)–Ru(1)–Ru(6)	92.75(3)	Ru(6)–P(1)–C(14)	120.24(23)
Ru(2)–Ru(3)–Ru(4)	64.82(3)	Ru(6)–P(1)–C(20)	111.10(20)
Ru(2)–Ru(4)–Ru(3)	57.767(25)	Ru(6)–P(1)–C(26)	113.29(21)
Ru(2)–Ru(4)–Ru(5)	91.73(3)	S(1)–Ru(2)–S(2)	85.61(6)
Ru(2)–S(1)–Ru(4)	73.98(5)	S(2)–C(1)–N(1)	114.5(5)
Ru(2)–S(2)–Ru(4)	73.97(5)	S(2)–C(1)–N(2)	120.3(5)
Ru(2)–S(2)–C(1)	103.87(23)	N(2)–C(1)–N(1)	125.2(6)
Ru(3)–Ru(2)–Ru(4)	57.415(24)	C(1)–N(2)–C(8)	119.3(6)

bond lengths vary significantly among bonds of the same order,[16] the distance between Ru1 and Ru2 clearly does not allow for a formal Ru–Ru bond. Lengthening of M–M bonds in cluster complexes upon substitution of a CO with the more basic phosphine has been noted previously[17] and demonstrates the inherent weakness of the Ru1–Ru2 interaction. Within the Ru1–Ru5–Ru6 triangular substructure, the sequence of long–short bond lengths has changed with respect to that of **1**,

(14) Hoferkamp, L.; Rheinwald, G.; Stoeckli-Evans, H.; Süss-Fink, G. *Organometallics* **1995**, in press.
(15) Beguin, A.; Rheinwald, G.; Stoeckli-Evans, H.; Süss-Fink, G. *Helv. Chim. Acta* **1994**, *77*, 525.
(16) Johnson, B. F. G.; Rodgers, A. In *The Chemistry of Metal Cluster Complexes*; Shriver, D. F., Kaesz, H. D., Adams, R. D., Eds.; VCH Publishers Inc.: New York, 1990; Chapter 6.
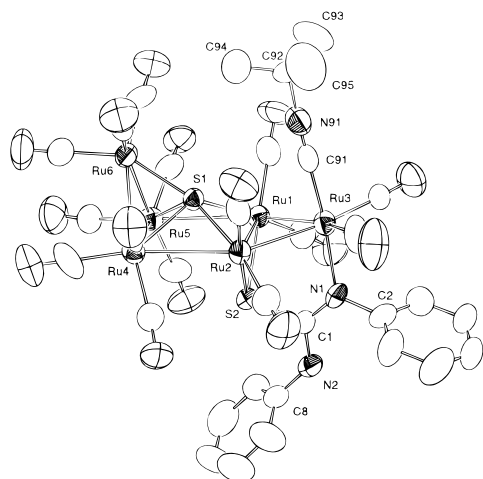
Figure 2. Molecular structure of **8**.

further suggesting alterations in the Ru−Ru bonding scheme. The Ru1−Ru6 vector elongates by *ca.* 0.17 Å, while Ru1−Ru5 shortens by *ca.* 0.13 Å. However, these changes do not affect the proposed M−M bond orders among those bonds. In opening the Ru1−Ru2 bond, the cluster now assumes the appearance of two trinuclear units linked through the μ_5-S and a single long, but not unreasonable, Ru−Ru bond (Ru4−Ru5, 3.0870(11) Å).

Although a bridging hydride could not be located in a difference map, the NMR data are consistent with the placement of this ligand spanning the Ru1−Ru5 vector; no coupling to the phosphorus atom is observed. As stated earlier, room temperature ^{1}H NMR spectra of **3** show a broad, poorly defined peak in the hydride region. Low temperature spectra, on the other hand, reveal two closely spaced peaks in an approximately 1:1 ratio. The two separate peaks, centered at −17.72 ppm (CD$_2$Cl$_2$, 400 MHz), reflect the presence of two isomers in solutions of **3**. One of these isomers (**3a**, $\delta = -17.70$ ppm) is believed to have the same structure as that observed in the solid state (Figure 2), with the PPh$_3$ ligand on Ru6 directed away from the bridging hydride. The second isomer (**3b**, $\delta = -17.73$ ppm) presumably contains the PPh$_3$ ligand at the same ruthenium atom (Ru6), but directed toward the bridging hydride.

With seven Ru−Ru bonds, the cluster **3** requires 94 electrons to achieve electronic saturation. No changes in the bond lengths or angles of the diphenylthioureato ligand indicate an alteration in its role as a five-electron donor. The same is true for the sulfur ligand, which continues to donate all six of its electrons to the cluster. Like the CO ligands, PPh$_3$ is a two-electron donor. Overall, cluster **3** contains 92 electrons, the same number as **1**; thus, it must be considered an electronically unsaturated cluster.

When exposed to CO, **3** does not reform **1**. Instead, cluster fragmentation occurs to generate the trinuclear species $(\mu_2$-H)Ru$_3$(CO)$_9(\mu_3,\eta^2$-SCNHPhNPh).[18] Presumably, the CO coordinates at the highly unsaturated Ru2, causing the Ru2−S1 bond to open. Further bond scission must follow, with the eventual abstraction of an ambient hydride to produce the trinuclear species.

Reactions of 1 with Other Two-Electron-Donor Ligands. In contrast to reactions of **1** with PPh$_3$,

(17) Bruce, M. I.; Liddell, M. J.; Hughes, C. A.; Skelton, B. W.; White, A. H. *J. Organomet. Chem.* **1988**, *347*, 157.
(18) Bodensieck, U.; Stoeckli-Evans, H.; Süss-Fink, G. *Chem. Ber.* **1990**, *123*, 1603.

Table 3. Selected Bond Lengths (Å) and Angles (deg) for 8

Ru(1)−Ru(2)	2.929(2)	Ru(4)−S(1)	2.394(3)
Ru(1)−Ru(3)	2.728(2)	Ru(5)−Ru(6)	2.784(2)
Ru(1)−Ru(5)	3.190(2)	Ru(5)−S(1)	2.393(3)
Ru(1)−S(1)	2.392(3)	Ru(6)−S(1)	2.312(3)
Ru(1)−S(2)	2.420(3)	S(2)−C(1)	1.802(12)
Ru(2)−Ru(3)	2.720(2)	N(1)−C(1)	1.28(2)
Ru(2)−Ru(4)	3.152(2)	N(1)−C(2)	1.45(2)
Ru(2)−S(1)	2.401(3)	N(2)−C(1)	1.34(2)
Ru(2)−S(2)	2.417(3)	N(2)−C(8)	1.44(2)
Ru(3)−N(1)	2.166(11)	N(91)−C(92)	1.49(2)
Ru(3)−C(91)	1.96(2)	C(91)−N(91)	1.14(2)
Ru(4)−Ru(5)	2.907(2)	C(98)−C(97)	1.70(6)
Ru(4)−Ru(6)	2.783(2)		

Ru(1)−Ru(2)−Ru(4)	90.56(4)	Ru(6)−Ru(5)−Ru(4)	58.50(4)
Ru(1)−S(1)−Ru(2)	75.34(9)	Ru(6)−S(1)−Ru(1)	142.29(14)
Ru(1)−S(1)−Ru(4)	129.22(14)	Ru(6)−S(1)−Ru(2)	142.35(14)
Ru(1)−S(1)−Ru(5)	83.64(10)	Ru(6)−S(1)−Ru(4)	72.49(9)
Ru(2)−Ru(1)−Ru(5)	89.04(4)	Ru(6)−S(1)−Ru(5)	72.56(9)
Ru(2)−Ru(3)−Ru(1)	65.04(4)	S(1)−Ru(1)−S(2)	85.50(11)
Ru(2)−S(2)−Ru(1)	74.53(10)	S(1)−Ru(2)−S(2)	85.36(11)
Ru(3)−Ru(1)−Ru(2)	57.35(4)	N(1)−C(1)−S(2)	118.7(9)
Ru(3)−Ru(1)−Ru(5)	145.65(5)	N(1)−C(1)−N(2)	125.8(11)
Ru(3)−Ru(2)−Ru(1)	57.62(4)	N(2)−C(1)−S(2)	115.6(10)
Ru(3)−Ru(2)−Ru(4)	147.09(5)	N(91)−C(91)−Ru(3)	179.5(13)
Ru(4)−Ru(5)−Ru(1)	90.20(4)	N(91)−C(92)−C(94)	106.3(14)
Ru(4)−Ru(6)−Ru(5)	62.96(4)	N(91)−C(92)−C(95)	107(2)
Ru(4)−S(1)−Ru(2)	82.20(10)	N(91)−C(92)−C(93)	108(2)
Ru(5)−Ru(4)−Ru(2)	90.17(4)	C(1)−N(1)−Ru(3)	123.2(8)
Ru(5)−S(1)−Ru(2)	127.26(14)	C(1)−N(1)−C(2)	117.9(11)
Ru(5)−S(1)−Ru(4)	74.80(10)	C(1)−N(2)−C(8)	127.5(11)
Ru(6)−Ru(4)−Ru(2)	97.25(4)	C(2)−N(1)−Ru(3)	118.9(9)
Ru(6)−Ru(4)−Ru(5)	58.54(4)	C(91)−Ru(3)−Ru(1)	87.9(4)
Ru(6)−Ru(5)−Ru(1)	96.08(4)	C(91)−N(91)−C(92)	177(2)

addition of P(n-Bu)$_3$, either of the phosphites P(OMe)$_3$ or P(OPh)$_3$, (CH$_3$)$_2$S, or ^{t}BuNC gives, as the major product, an intact, monosubstituted derivative of **1**, $(\mu_2$-H)Ru$_6$(CO)$_{15}$(L)$(\mu_5$-S)$(\mu_3,\eta^2$-SCNHPhNPh) [L = P(n-C$_4$H$_9$)$_3$ (**4**), L = P(OMe)$_3$ (**5**), L = P(OPh)$_3$ (**6**), L = (CH$_3$)$_2$S (**7**), and L = (CH)$_3$CNC (**8**)]. The duration of
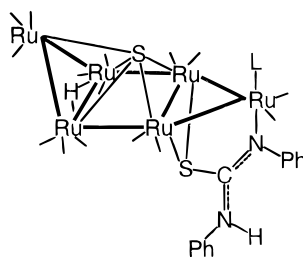
	L
4	Me$_2$S
5	P(n-Bu)$_3$
6	P(OMe)$_3$
7	P(OPh)$_3$
8	^{t}BuNC

the reaction has very little effect on the product yields. These derivatives are all easily isolated by using preparative TLC. Spectral data (see Experimental Section) clearly show that the site of substitution in these derivatives differs from that of **3**. Insignificant spectral shifts of relevant signals for the diphenylthioureato ligand, as compared to the same data for **1**, establish its bonding mode as unchanged. Only in the case of cluster **8** do the NH and CH$_3$ signals in the ^{1}H NMR spectra indicate the presence of isomers.

Verification of the site of substitution in **4**−**8** was provided by structural analysis of the ^{t}BuNC-substituted derivative, **8**. Deep red plates of **8** could be isolated from 3:1 acetone/heptane solutions maintained at 5 °C for 3 days. These crystals were triclinic of the space group $P\bar{1}$. Additional crystal data are summarized in Table 1. An Ortep plot of **8** is presented in Figure 2, and selected bond lengths and angles are given in Table 3. An area of disordered solvent was associated with each molecule of **8**.

The molecular structure of **8** shows a derivative of **1** resulting from CO substitution by the two-electron-

donor group ^{t}BuNC. The cluster skeleton of **8**, like that of **1**, consists of five Ru atoms arranged in a pentagonal-shaped polyhedron with a sixth Ru atom bridging the Ru−Ru edge opposite to the apex. The sixth Ru atom rises above the planar base at an angle of 85°. The pentacoordinate S remains bonded to five metal atoms, four from the square base (Ru1, Ru2, Ru4, and Ru5) and the out-of-plane, apical Ru atom (Ru6). The triangular substructure composed of Ru1, Ru2, and Ru3 is spanned by a μ_3,η^2-diphenylthioureato ligand. In contrast to the monosubstituted PPh$_3$ derivative **3**, the isonitrile ligand in **8** occupies an axial position on the in-plane apical Ru atom of the hexanuclear framework (Ru3). Previous studies of trinuclear ruthenium clusters containing μ_3,η^2-bridging ligands have shown regiospecific substitution of carbonyl groups at the bridged metal atoms,[19] but substitution at the metal bound to the nonbridging nitrogen atom of similar ligands is not unfounded.[20] The C91−N91−C92 pole of the ligand is almost perfectly vertical, bending slightly toward (∼2°) the interior of the cluster. Terminal carbonyl ligands are found on each of the Ru atoms. A bridging hydride could not be located in the refinement of the structural data of **8**, but the ^{1}H NMR spectral data show a single peak in the hydride region essentially unchanged from that of **1**. Thus, it is likely that a hydride ligand bridges the Ru4−Ru5 vector of **8** (Ru1−Ru5 in **1**).

The bond lengths and angles determined for **8** show little change from those of **1**. The two triangular substructures consist of Ru−Ru single bonds, wherein the multiply bridged sides (Ru4−Ru5 and Ru1−Ru2) are elongated relative to the remaining two bonds. The trinuclear units are connected by long Ru−Ru bonds (Ru1−Ru5 and Ru2−Ru4); however, the bond lengths lie within acceptable limits for Ru−Ru single bonds. As in the case of **1**, these interactions relieve the unsaturation predicted by standard electron counting rules at Ru1 and Ru2 (Ru2 and Ru4 in **1**). The noticeable changes in the analogous Ru−Ru bond lengths apparent upon comparison of **3** and **1** are absent from the derivative **8**.

The presence of isomers in solutions of **8**, as implied by the ^{1}H NMR spectrum, is due to differing orientations of the ^{t}BuNC group. The situation is similar to that described for **3**. Steric requirements should favor an orientation in which the ^{t}BuNC group occupies an axial coordinate site on Ru3, as determined crystallographically. The phenyl group on N2 would interact to a lesser extent with an axial ^{t}BuNC group than with that group in an equatorial position. This axial isomer produces the NH signal at 6.76 ppm and the CH$_3$ signal at 1.50 ppm. The isomer containing the ^{t}BuNC group in an equatorial coordination site still occurs, however, and is most likely responsible for the NH peak at 6.74 ppm and the CH$_3$ peak at 1.54 ppm. That binding still occurs in the equatorial isomer can be traced to the large separation between the N2-bound phenyl and the ^{t}Bu methyls provided by the C−N−^{t}Bu linkage. This situation is illustrated in Figure 3. No NMR evidence was found for the existence of isomers in solutions of **4−7**.

In an effort to gain insight into the nature of these substitution reactions, a series of variable temperature
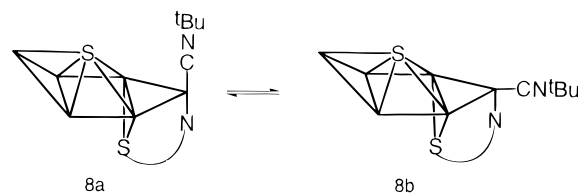
Figure 3. Axial−equatorial exchange of the isonitrile ligands of **8**.

^{31}P NMR experiments on the formation of compounds **3** and **7** was carried out. The ^{31}P NMR spectrum of a solution of **1** and P(OPh)$_3$, maintained at −50 °C, shows only the free ligand and a small amount of the substitution product, **7**. Subsequent spectra obtained at increasingly higher temperatures show the free ligand signal intensity to diminish and the signal corresponding to **7** to increase. At room temperature, only the signal corresponding to the monosubstituted product is found. From these data, it appears that the formation of **7** is straightforward and involves no intermediates. The reaction of **1** with any of P(n-Bu)$_3$, P(OMe)$_3$, Me$_2$S, or ^{t}BuNC is assumed to follow an analogous course.

In contrast, the formation of **3** is more complex. The −50 °C ^{31}P NMR spectrum of a solution of **1** and PPh$_3$ shows two signals, both in the region of metal-bound phosphine groups, neither of which corresponds to the substitution product **3**. If the solution is allowed to warm slowly, both of these signals deteriorate and others grow in, until at room temperature a series of signals associated with coordinated PPh$_3$ groups is observed as well as a signal for the free ligand. Additional spectra obtained over a period of 48 h show no indication of the product **3**. However, chromatographic workup of the test solution produces **3** in typical yields, suggesting that the monosubstituted product is formed during workup of the reaction solution, presumably on the TLC plates.

Conclusions

It is established that the weakest points in transition metal carbonyl clusters are the metal−metal bonds.[3] Reactions of the hexanuclear "sofa" cluster **1** with PPh$_3$ demonstrate the truly sensitive nature of these structural features. In this reaction, the effects of replacing CO with the isoelectronic PPh$_3$ manifest themselves in metal−metal bond length changes relatively far removed from the substitution site. Other two-electron-donor groups, including some alternative phosphorus-based reagents, also result in substitution, but not at the same Ru atom, and moreover, these ligands do not significantly affect the Ru framework relative to that of **1**. Steric interaction is most likely responsible for the variation in the site of substitution.

Experimental Section

Manipulations were carried out by using standard Schlenk techniques[21] under an N$_2$ atmosphere. Thermolysis reactions were performed in a high-pressure Schlenk tube able to withstand 8 bars of internal pressure. TLC plates were prepared by placing a uniform 0.5 mm layer of the appropriate support (Al$_2$O$_3$ or SiO$_2$, G or G/UV$_{254}$, Macherey-Nagel) on 20 × 20 cm glass plates. Laboratory solvents were purified and dried according to standard laboratory practices.[22] Distillation of solvents was carried out under an N$_2$ atmosphere; the inert atmosphere over the solvent was maintained thereafter. The

(19) (a) Andreu, P. L.; Cabeza, J. A.; Riera, V.; Bois, C.; Jeannin, Y. *J. Chem. Soc., Dalton Trans.* **1990**, 3347. (b) Andreu, P. L.; Cabeza, J. A.; Riera, V. *J. Organomet. Chem.* **1990**, *393*, C30.
(20) Cabeza, J. A.; Franco, R. J.; Llamazares, A.; Riera, V.; Pérez-Carreño, E.; Van der Maelen, J. F. *Organometallics* **1994**, *13*, 55.

(21) Herzog, S.; Dehnert, J. *Z. Chem.* **1969**, *4*, 1.
(22) Perrin, D. D.; Armarego, W. L. F. *Purification of Laboratory Chemicals*, 3rd ed.; Pergamon Press: Oxford, England, 1988.

cluster $(\mu_2\text{-H})Ru_6(CO)_{16}(\mu_5\text{-S})(\mu_3,\eta^2\text{-SCNHPhNPh})$ (**1**) was prepared according to a previously published procedure.[11d] Other chemicals [*tert*-butylisonitrile (Fluka, 98%), methyl sulfide (Fluka, 99%), tri-*n*-butylphosphine (Fluka, 99%), trimethyl phosphite (Fluka, 99%), triphenylphosphine (Merck, 98%), triphenyl phosphite (Fluka, 99%)] were purchased from the appropriate vendors and used as received. Infrared spectra were obtained by using a Perkin-Elmer 1720X spectrometer. Room temperature ^{1}H and ^{31}P NMR spectra were acquired with either a Bruker AMX 400 or a Varian Gemini 200 BB spectrometer, while all low temperature ^{31}P NMR spectra were acquired by using the Bruker AMX 400 instrument with controlled temperature nitrogen gas flow. Elemental analyses were performed by the Mikroelementaranalytisches Laboratorium der ETH, Zürich, Switzerland. FAB mass spectra were measured by Professor T. A. Jenny of the University of Fribourg, Fribourg, Switzerland, using 3-nitrobenzyl alcohol (NBA) as the matrix.

X-ray structural data were collected on a Stoe-Siemens AED 2 four-circle diffractometer using graphite-monochromatized Mo Kα radiation ($\lambda = 0.710\ 73$ Å). Low temperature measurements were carried out using controlled temperature nitrogen gas flow. Crystal structure data were solved by using SHELXS86[23] and refined by using either SHELXL93[24] or the NRCVAX[25] program packages of the VAX-Cluster of the Départment de Calcul de l'Université de Neuchâtel. Illustrations showing thermal motion ellipsoids were drawn by using either the PLATON[26] or ZORTEP[27] program. Additional data for structures have been deposited with the Cambridge Crystallographic Data Centre, Union Road, GB-Cambridge CB2 1EW, UK.

Syntheses of $Ru_2(CO)_4(PPh_3)_2(\mu_2,\eta^2\text{-SCNHPhNPh})$ (2) and $(\mu_2\text{-H})Ru_6(CO)_{15}(PPh_3)(\mu_5\text{-S})(\mu_3,\eta^2\text{-SCNHPhNPh})$ (3). A solution of **1** (64 mg, 0.049 mmol) and PPh$_3$ (26.8 mg, 0.102 mmol) in C$_6$H$_{12}$ (20 mL) was stirred for 24 h. The solvent was removed, the residue was dissolved in CH$_2$Cl$_2$, and the products were separated by TLC (Al$_2$O$_3$, 40:60 Et$_2$O/cyclohexane). Compound **2** was isolated from a leading yellow band (<3% yield), while compound **3** was isolated from a red brown band (29 mg, 38.2%) located just below a faint red band consisting of the trinuclear compound $Ru_3(CO)_6(\mu_2\text{-}C_6H_5)(\mu_2\text{-}PPh_2)(\mu_3,\eta^2\text{-SCNHPhNPh})$[14] (trace). Crystals of **3** were grown at room temperature from a 3:1 CH$_2$Cl$_2$/C$_7$H$_{16}$ solution. Spectroscopic and analytical data for **2**: IR (c-hex, 298 K, ν_{CO} (cm^{-1})) 2019vs, 1987m, 1956s; IR (KBr, ν_{NCN} (cm^{-1})) 1624m, 1588m; ^{1}H NMR (CDCl$_3$ 298 K, 200 MHz) δ 7.48–6.85 (m, 25H, Ph-*H*), 5.72 (s, br, 1H, N-*H*); ^{31}P NMR (CDCl$_3$, 298 K) δ 24.47 (s). Anal. Calcd for C$_{66}$H$_{52}$N$_4$O$_4$P$_2$Ru$_2$S$_2$·CH$_2$Cl$_2$ (1378): C, 58.39; H, 3.95; N, 4.06. Found: C, 59.0; H, 4.17; N, 2.77. Spectroscopic and analytical data for **3**: IR (c-hex, 298 K, ν_{CO} (cm^{-1})) 2061vs, 2040s, 2004s, 1989w,br, 1943m,br; IR (KBr, ν_{NH} (cm^{-1})) 3333m; IR (KBr, ν_{NCN} (cm^{-1})) 1564m; ^{1}H NMR (CDCl$_3$, 298 K, 200 MHz) δ 7.60–7.07 (m, 25H, Ph-*H*), 6.74 (s, br, 1H, N-*H*), −17.50 (s, br, 1H, Ru$_2$-*H*); ^{31}P NMR (CDCl$_3$, 298 K) δ 34.48(s). Anal. Calcd for C$_{46}$H$_{28}$N$_2$O$_{15}$PRu$_6$S$_2$ (1550.3): C, 35.64; H, 1.82; N, 1.81. Found: C, 35.92; H, 1.62; N, 1.86.

Syntheses of $(\mu_2\text{-H})Ru_6(CO)_{15}(\mu_5\text{-S})(Me_2S)(\mu_3,\eta^2\text{-SCN-HPhNPh})$ (4). A solution of **1** (30 mg, 0.023 mmol) and Me$_2$S (0.075 mmol) in CH$_2$Cl$_2$ (10 mL) was stirred at room temperature for 7 days. After removal of the solvent, the residue was redissolved in CH$_2$Cl$_2$ and chromatographed on Al$_2$O$_3$ TLC plates in 1:3 CH$_2$Cl$_2$/cyclohexane. The first band contained unreacted **1**, while the dark red band just below that contained **4** (12.6 mg, 40.6%). Spectral and analytical data for **4**: IR (c-hex, 298 K, ν_{CO} (cm^{-1})) 2085m, 2058vs, 2043s, 2026vs, 2013w, 2002m, 1988m, 1981w, 1956m, 1930w; IR (KBr, ν_{NH} (cm^{-1})) 3355m; IR (KBr, ν_{NCN} (cm^{-1})) 1565m; ^{1}H NMR (CDCl$_3$, 298 K, 200 MHz) δ 7.10−7.70 (m, 10H, Ph-*H*), 6.85 (s, br, 1H, N-*H*), 2.06 (s, 6H, CH$_2$-*H*); FAB-MS (NBA) M$^+$, 1349. Anal. Calcd for C$_{30}$H$_{18}$N$_2$O$_{15}$Ru$_6$S$_3$ (1353.4): C, 26.71; H, 1.34; N, 2.08. Found: C, 26.58; H, 1.50; N, 1.98.

Syntheses of $(\mu_2\text{-H})Ru_6(CO)_{15}(L)(\mu_5\text{-S})(\mu_3,\eta^2\text{-SCNHPh-NPh})$ [L = P(n-C$_4$H$_9$)$_3$ (5), P(OMe)$_3$ (6), P(OPh)$_3$ (7), (CH)$_3$-CNC (8)]. A solution of **1** (**5**, 59 mg, 0.045 mmol; **6**, 33.5 mg, 0.025 mmol; **7**, 67.4 mg, 0.051 mmol; **8**, 62.0 mg, 0.047 mmol) in a solvent (cyclohexane, CH$_2$Cl$_2$, or THF produced similar results) (20 mL) was prepared in a dried Schlenk tube. Under N$_2$ flow, a solution of the appropriate reagent [**5**, P(n-C$_4$H$_9$)$_3$, 12.0 μL, 0.048 mmol; **6**, P(OMe)$_3$, 3.0 μL, 0.027 mmol; **7**, P(OPh)$_3$, 14 μL, 0.054 mmol; **8**, (CH)$_3$CNC, 6 μL, 0.053 mmol] in the appropriate solvent (10 mL) was added dropwise to the stirring solution. The solution color immediately turned a deeper shade of red. The reaction solution was stirred at room temperature for 4−6 h. After removal of the solvent, the residue was redissolved in CH$_2$Cl$_2$ and chromatographed on TLC plates (Al$_2$O$_3$, 40:60 Et$_2$O/cyclohexane). Compounds **5**−**8** were isolated from prominent red bands located in the lower half of the TLC plates: **5**, 15.3 mg, 22.8%; **6**, 12.2 mg, 34.0%; **7**, 53.4 mg, 65.2%; **8**, 37.0 mg, 53.0%. Samples for elemental analyses were prepared by recrystallization of the products from CH$_2$Cl$_2$ layered with an excess of hexane or heptane. Spectral and analytical data for **5**: IR (c-hex, 298 K, ν_{CO} (cm^{-1})) 2083m, 2056vs, 2041s, 2023vs, 2011w, 2001m, 1985m,br, 1953m, 1925w; IR (KBr, ν_{NH} (cm^{-1})) 3362m; IR (KBr, ν_{NCN} (cm^{-1})) 1552m; ^{1}H NMR (CDCl$_3$, 298 K, 200 MHz) δ 7.40−7.10 (m, Ph-*H*), 6.81 (s, br, N-*H*), 1.43−0.84 (m, C$_4$H$_9$), −22.07 (s, Ru$_2$-*H*); ^{31}P NMR (CDCl$_3$, 298 K) δ 20.81(s); FAB-MS (NBA) M$^+$, 1486. Anal. Calcd for C$_{40}$H$_{38}$N$_2$O$_{15}$PRu$_6$S$_2$·1/2C$_6$H$_{14}$ (1535.6): C, 33.6; H, 2.95; N, 1.82. Found: C, 33.0; H, 3.03; N, 2.29. Spectral and analytical data for **6**: IR (c-hex, 298 K, ν_{CO} (cm^{-1})) 2084m, 2057vs, 2041s, 2030s, 2015m, 2001m, 1989m, 1966w, br, 1937w,br; IR (KBr, ν_{NH} (cm^{-1})) 3339m; IR (KBr, ν_{NCN} (cm^{-1})) 1554m; ^{1}H NMR (CDCl$_3$, 298 K, 200 MHz) δ 7.57−7.10 (m, 10H, Ph-*H*), 6.78 (s, br, 1H, N-*H*), 3.45 (d, $J = 11.2$ Hz, 9H, CH$_2$-*H*), −22.0 (s, 1H, Ru$_2$-*H*); ^{31}P NMR (CDCl$_3$, 298 K) δ 121.8(s); FAB-MS (NBA) M$^+$, 1409. Anal. Calcd for C$_{31}$H$_{21}$N$_2$O$_{18}$PRu$_6$S$_2$ (1411.0): C, 26.4; H, 1.50; N, 1.99. Found: C, 27.15; H, 1.58; N, 2.05. Spectral and analytical data for **7**: IR (c-hex, 298 K, ν_{CO} (cm^{-1})) 2085m, 2058vs, 2042s, 2031s,sh, 2016m, 2002m, 1990m, 1976w,br, 1942w,br; IR (KBr, ν_{NH} (cm^{-1})) 3355m; IR (KBr, ν_{NCN} (cm^{-1})) 1556m; ^{1}H NMR (CDCl$_3$, 298 K, 200 MHz) δ 7.43−6.67 (m, 25H, Ph-*H*), 6.78 (s, br, 1H, N-*H*), −22.1 (s, 1H, Ru$_2$-*H*); ^{31}P NMR (CDCl$_3$, 298 K) δ 107.7(s); FAB-MS (NBA) M$^+$, 1598. Anal. Calcd for C$_{46}$H$_{27}$N$_2$O$_{18}$PRu$_6$S$_2$ (1597.2): C, 34.6; H, 1.70; N, 1.75. Found: C, 34.8; H, 1.69; N, 1.72. Spectral and analytical data for **8**: IR (c-hex, 298 K, ν_{NC} (cm^{-1})) 2166w; IR (c-hex, 298 K, ν_{CO} (cm^{-1})) 2084m, 2057vs, 2042s, 2033s, 2016m, 2001m, 1989s,br, 1976w,br, 1939w,br; IR (KBr, ν_{NH} (cm^{-1})) 3361w; IR (KBr, ν_{NCN} (cm^{-1})) 1564m; ^{1}H NMR (CDCl$_3$, 298 K, 200 MHz) δ 7.60−7.12 (m, 10H, Ph-*H*), 6.76 (s, br, 0.8H), 6.74 (s, br, 0.2H, N-*H*), 1.54 (s, 0.2H) 1.50 (s, 0.8H, C-*H*$_3$), −21.91 (s, 1H, Ru$_2$-*H*). Anal. Calcd for C$_{33}$H$_{21}$N$_3$O$_{15}$S$_2$Ru$_6$·0.5C$_7$H$_{16}$ (1420.1): C, 30.87; H, 2.06; N, 2.96. Found: C, 29.92; H, 2.02; N, 2.96.

Supporting Information Available: Tables of positional and thermal parameters, bond lengths and angles, and least squares planes for **3** and **8** (18 pages). Ordering information is available on any current masthead page.

OM950739V

(23) Sheldrick, G. M. *SHELXS-86, Program for Crystal Structure Determination*; University of Göttingen: Göttingen, Germany, 1986.
(24) Sheldrick, G. M. *SHELXL-93, Program for Refinement of Crystal Structure Data*; University of Göttingen: Göttingen, Germany, 1993.
(25) Gabe, E. J.; Le Page, Y.; Charland, J.-P.; Lee, F. L. NRCVAX−an Interactive Program System for Structure Analysis. *J. Appl. Crystallogr.* **1989**, *22*, 384.
(26) Spek, A. L. *Acta Crystallogr.* **1990**, *A46*, C34.
(27) Johnson, C. K. *ORTEP*; Oak Ridge National Laboratory: Oak Ridge, TN [modified for PC (ZORTEP) by L. Zsolnai and H. Pritzkow, University of Heidelberg, Heidelberg, Germany, 1994].